Oxidative properties and utility of fabricated $MnSiO_3$ nanoparticles for colorimetric detection of iron (II) in water samples

Tao Wang, Haoran Jiang, Qiang Bai, Hailian Xiao, Manhong Liu, Ning Sui ✉

College of Materials Science and Engineering, Qingdao University of Science and Technology, Qingdao 266042, People's Republic of China
✉ *E-mail: suining@qust.edu.cn*

Published in Micro & Nano Letters; Received on 7th September 2019; Revised on 8th February 2020; Accepted on 2nd June 2020

$MnSiO_3$ nanoparticles (NPs) were prepared by precipitation method, their structure and composition were characterised by transmission electron microscopy, electron diffraction spectroscopy, X-ray diffraction, and X-ray photoelectron spectroscopy. Due to the oxidase-like enzyme activity of $MnSiO_3$, it can catalyse the substrate 3,3′,5,5′-tetramethylbenzidine (TMB) in acidic environment to form an oxidised TMB which has an absorption peak at 652 nm in the absence of hydrogen peroxide. When Fe^{2+} was added to the assay, the oxidase-like activity of $MnSiO_3$ was inhibited, and the intensity of the absorption at 652 nm was reduced. Based on the high oxidase-like activity, a colorimetric method for Fe^{2+} detection was established, it showed high selectivity and sensitivity. In the optimised conditions, the limit of detection was 0.5 μM with a linear range from 3 to 63 μM. Moreover, the method was applied to determine Fe^{2+} in spiked water samples which gave satisfactory recoveries.

1. Introduction: Colorimetric method has been widely accepted with great potential in portable and inexpensive daily applications [1]. With the development of this research field, enzyme-mimetic nanomaterials have been widely used in detecting H_2O_2 [2], glucose [3]. Compared with natural enzymes, synthetic nanozymes such as PtCu nanowires [4] are highly stable and low-cost. Unfortunately, some shortcomings, such as poor reproducibility and complex preparation process of the nanozymes still need to be improved.

3,3′,5,5′-Tetramethylbenzidine (TMB) is widely used as a chromogenic substrate in immunohistochemistry, enzyme-linked immunosorbent assays and other detections [5]. TMB can be oxidised into different forms of charge-transfer complex in the presence of peroxidase or oxidase enzymes, generating a yellow, blue or green colour solution [6]. Although the TMB-H_2O_2-horseradish peroxidase (HRP) detection system has been widely used in analytical detections, it still has disadvantages. For instance, H_2O_2 is important to the oxidation of TMB, whereas it has a short-term storage stability and temperature instability, limiting its practical application. Accordingly, development of H_2O_2-free detection systems is highly preferable.

Fe^{2+} plays an important role in biology, industry, and the natural environment. High level of Fe^{2+} in drinking water may cause the respiratory tract damage, cough and shortness of breath, kidney failure, liver damage, skin damage, and even death [7], so the detection of Fe^{2+} is an important issue. So far, some detection methods have been reported. Chen *et al.* designed $CePO_4$: Tb^{3+} nanocrystal-H_2O_2 hybrid system with synchronous fluorescence scan technique, providing a fluorimetry method for selective detection of Fe^{2+} [8]. Compared with those detection methods, colorimetric method has a better potential for practical applications for its low-cost and efficient coreactants [9], it is necessary to explore a method for detecting Fe^{2+} with simple process, sensitivity, and high selectivity.

In this work, we firstly report the oxidase-like activity of $MnSiO_3$ nanoparticles (NPs), and a sensitive $MnSiO_3$ NPs-TMB chromogenic system for detection of Fe^{2+} was proposed. $MnSiO_3$ catalyses the oxidation of TMB to generate a typical cyan colour, with the addition of Fe^{2+}, oxidised TMB (oxTMB) is reduced into TMB, accompanying obviously colour change from blue to colourless. The detection procedure is illustrated in Fig. 1. In the optimised conditions, the sensitivity and selectivity were investigated. Moreover, the application of this assay for detecting Fe^{2+} in spiked water samples was investigated.

2. Materials and methods: Manganese acetate ($Mn(CH_3COO)_2$) was purchased from MeiXing Chemical Reagent Co. Ltd (Shanghai, China). Sodium silicate (Na_2SiO_3) was purchased from HengXing Chemical Reagent Co. Ltd (Tianjin, China). Hexadecyl trimethyl ammonium bromide (CTAB), citric acid ($C_6H_8O_7$), and disodium phosphate (Na_2HPO_4) were purchased from BoDi Chemical Reagent Co. Ltd (Tianjin, China). 3,3′ 5,5′-tetr-amethylbenzidine (TMB) was purchased from JinSui Chemical Reagent Co. Ltd (Shanghai, China). All the chemicals were of analytical grade and used as received without any purification. The solutions were prepared with ultrapure water.

Powder X-ray diffraction (XRD) patterns of $MnSiO_3$ were obtained using a D/MAX-2500/PC diffractometer (Rigaku, Japan) using Cu-Kα radiation. UV–visible absorption spectra (UV–Vis) were recorded on a Hitachi U-3900H UV–Vis spectrophotometer at room temperature. The surface elemental composition and oxidation state of the products were obtained by a Thermo-ESCALAB 250XI (Thermo, USA) instrument with non-monochromated Al-Kα radiation. A FEI Tecnai G2 F20 transmission electron microscope (TEM) was employed to observe the morphology of the $MnSiO_3$.

$MnSiO_3$ NPs were synthesised according to the previously published procedure [10]. Typically, 0.245 g $Mn(CH_3COO)_2{\cdot}4H_2O$ was dissolved in 20 ml ultrapure water, 0.284 g $Na_2SiO_3{\cdot}9H_2O$ was dissolved in 10 ml ultrapure water. In a round bottom flask, 0.364 g CTAB was dissolved in 20 ml ultrapure water. Then, Na_2SiO_3 solution and $Mn(CH_3COO)_2$ solution were added to the CTAB solution and constantly stirred for 1 h. The mixture was incubated at room temperature (25°C) for 8 h. The precipitate was collected by centrifugation and washed twice with distilled water and ethanol, respectively. Finally, the precipitate was dried at 60°C for 12 h under vacuum.

Fe^{2+} detection was conducted as follows, 3 ml disodium hydrogen phosphate-citric acid buffer (pH = 4.0), TMB (0.06 mM), and $MnSiO_3$ (0.06 mg/ml) were placed in an conical bottle. After shaking, the solution was incubated at room temperature (25°C) for 15 min, different concentrations of Fe^{2+} solutions were added.

doi: 10.1049/mnl.2019.0543

Then, UV–Vis spectrophotometer was used for analysis of the solution, and the corresponding absorption spectra was obtained.

The real-world samples were taken from the lake in Zhangjiajie Natural Scenic Spot (Hunan, China). The sample was not treated before determination. The resulting lake water was filtered and diluted 20-fold with deionised water. After that, the diluted lake water was spiked with different standard solutions of Fe^{2+} (25, 45, and 60 μM). Finally, the experiment was conducted according to the above detection method.

3. Results and discussion: TEM was used to obtain the detailed morphology and structure information of the as-prepared $MnSiO_3$. TEM image shows an irregular shape of $MnSiO_3$ NPs was obtained and the $MnSiO_3$ colloid was reddish brown (Fig. 2*a*), which indicated well-dispersed $MnSiO_3$ NPs. The three elemental mapping images demonstrate that the as-prepared product consists of Mn, Si, and O, and these three elements are evenly distributed (Fig. 2*b*). The XRD patterns of the $MnSiO_3$ are revealed in Fig. 2*c*. The absence of any distinguishable diffraction peaks in the patterns indicates the as-prepared products are amorphous. X-ray photoelectron spectroscopy (XPS) was used to identify the chemical state and surface nature of the as-prepared $MnSiO_3$. The high resolution Mn 2p spectrum in Fig. 2*d* includes two typical peaks around 642.2 eV (Mn $2p_{3/2}$) and 653.6 eV (Mn $2p_{1/2}$) [11], which could be, respectively, segmented into three peaks. The peaks at 641.9 and 653.4 eV result from the Mn^{2+} in $MnSiO_3$ [12], those at 642.0 and 653.7 eV from Mn^{3+} [13], and those at 642.6 and 653.9 eV from Mn^{4+} [11]. Mn^{2+} is easy to be oxidised to Mn^{3+} and Mn^{4+} in water solution.

The detection strategy for Fe^{2+} is based on the enzyme-like activity of the $MnSiO_3$ NPs. To investigate the oxidase activity of the $MnSiO_3$ NPs, TMB was used as the oxidase substrate to study the catalytic oxidation reaction in the absence of H_2O_2. As shown in Fig. 3, the as prepared $MnSiO_3$ NPs could catalyse the oxidation of TMB in the absence of H_2O_2 to produce a typical blue-green colour, indicating the formation of blue one-electron oxidation product, 3,3′,5,5′-tetramethylbenzidine diimine (TMBDI). Compared with the control experiments without $MnSiO_3$ NPs, $MnSiO_3$-TMB system generated the deepest colour. Accordingly, this obvious absorbance value at 652 nm was also monitored by the UV–Vis absorption spectroscopy. O-phenylenediamine (OPD) and 2,2′-azino-bis (3-ethylbenzothiazoline-6-sulfonic acid) (ABTS) as two typical oxidase substrates were used to replace TMB (Fig. 3*c*). OPD and ABTS generated strong absorption peaks in the UV–vis spectrum, respectively. All of the above results confirm that the as-synthesised $MnSiO_3$ possesses an intrinsic oxidase-like catalytic activity. Nevertheless, when Fe^{2+} was added, the $MnSiO_3$-TMB system was inhibited in the colour of the solution faded and the absorption peak disappeared, because oxTMB was reduced. Hence, a low-cost, and sensitive assay is achieved for visual colorimetric detection of Fe^{2+}. The detection mechanism can be explained by the following reaction formula [14]:

$$Mn^{2+} + O_2 \rightarrow Mn^{3+} + O_2^{\cdot -} \quad (1)$$

$$O_2^{\cdot -} + H^+ + Mn^{2+} \rightarrow Mn^{3+} + OH^- + OH^{\cdot} \quad (2)$$

According to XPS results, $MnSiO_3$ NPs possess the oxidation states Mn^{2+}/Mn^{3+}, and Mn^{2+} transfers electrons to O_2 causing the formation of superoxide anions ($O_2^{\cdot -}$) [14, 15]. It has been proved that $O_2^{\cdot -}$ produce H_2O_2 partly by non-enzymatic or SOD-catalysed dismutation. Then, Mn^{2+} reacts with H_2O_2 to produce hydroxyl radicals ($OH^{\cdot}$) [16, 17]. The oxidation environment

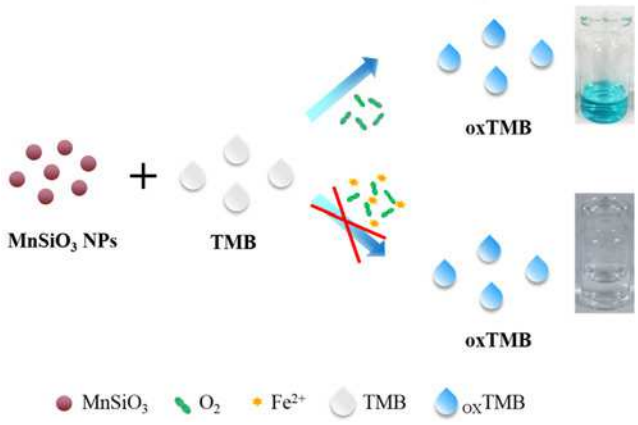

Fig. 1 *Scheme of the sensing system for Fe^{2+} detection*

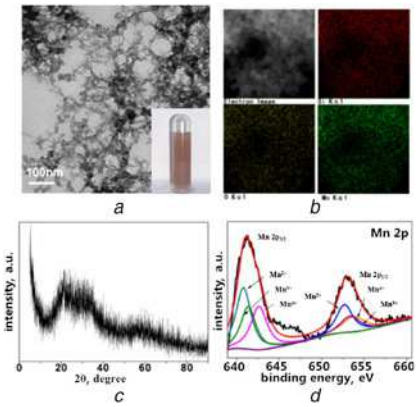

Fig. 2 *Characterisation of $MnSiO_3$*
a TEM images of $MnSiO_3$ NPs
b Elemental mappings for Mn, Si, and O in the as-prepared $MnSiO_3$
c XRD pattern of the as-obtained of $MnSiO_3$ NPs
d XPS survey spectra of Mn 2p of $MnSiO_3$

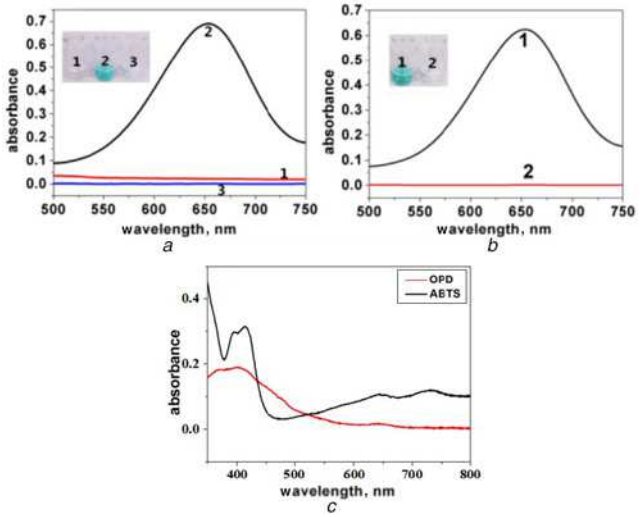

Fig. 3 *Oxidase activity of $MnSiO_3$*
a UV–Vis absorption of (1) 0.06 mM TMB solution, and $MnSiO_3$ NPs (0.06 mg/ml)-TMB chromogenic system in the (2) absence and (3) presence of 0.08 mM Fe^{2+}
b UV–Vis absorbance spectra and visual colour changes of TMB (1) with O_2 or (2) without O_2
c $MnSiO_3$ catalyses the oxidation of different substrates to produce various absorption peaks

includes $O_2^{\cdot-}$/OH$^{\cdot}$ and Mn^{3+}, oxidising TMB to show the blue colour. In order to validate the mechanism, the solution was bundled with high purity nitrogen to remove dissolved oxygen for 15 min before adding $MnSiO_3$ NPs. From Fig. 3*b* we can deduce that $O_2^{\cdot-}$ radicals and some OH$^{\cdot}$ radicals were generated because of the presence of oxygen. The results were well matched with the mechanism above mentioned, that is, in the presence of $MnSiO_3$ NPs, dissolved oxygen participated in the system and thus produced the oxygen free radicals, which further confirmed that the assay can be carried out without adding H_2O_2.

In order to optimise the detection condition, reaction times, pH values, and concentrations of TMB and $MnSiO_3$ were investigated. The optimal pH for $MnSiO_3$ is 4.0, which is similar to HRP [6] (Fig. 4*a*). The nature of pH dependent catalytic activity chiefly rely on the chromogenic substrate itself rather than the enzymes. Fig. 4*b* shows the influence of reaction time, it can be seen that the absorption peak at 652 nm increased as the reaction time increased from 1 to 15 min, and with the reaction time being longer than 15 min, the absorption peak did not change significantly. Therefore, 15 min was considered to be the best reaction time in our experiments. As shown in Fig. 4*c*, the strong absorbance peak at 652 nm gradually increased with an increase in the concentration of $MnSiO_3$. Furthermore, an increase in the concentration of $MnSiO_3$ leads to an increase in the catalytic activity. Fig. 4*d* show that the UV absorption peaks of the system increased with the increase of TMB concentration. Measurement errors exist in photometric analysis, especially in UV–Vis photometric analysis. According to Lambert Beer's law, the errors of transmittance and absorbance are the main factor to evaluate the measurement result. In the actual measurement, only the transmittance (T) to be measured is between 15 and 65%, or the absorbance (A) is between 0.2 and 0.8, can ensure the relative error of measurement to be less than 4% [18–20]. To ensure the accuracy and the catalytic activity of $MnSiO_3$, the following experimental conditions were adopted: (i) 0.06 mg/ml $MnSiO_3$; (ii) 0.06 mM TMB.

Under the optimal conditions, different experiments were carried out, including dynamic range, sensitivity, and selectivity of this chromogenic system was evaluated for detection of Fe^{2+}. As shown in Fig. 5*a*, the absorbance at 652 nm gradually decreased as the concentration of Fe^{2+} varied from 0 to 0.5 mM. The inset in Fig. 5*b* shows a linear correlation between the absorption peak at 652 nm and the Fe^{2+} concentration, ranging from 3 to 63 µM.

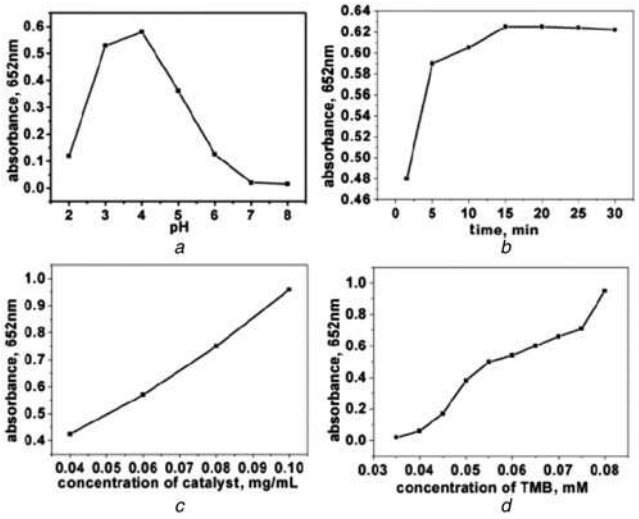

Fig. 4 *Dependences of the oxidase-like activity of $MnSiO_3$ on*
a pH
b Reaction time
c Concentrations of $MnSiO_3$
d Concentrations of TMB

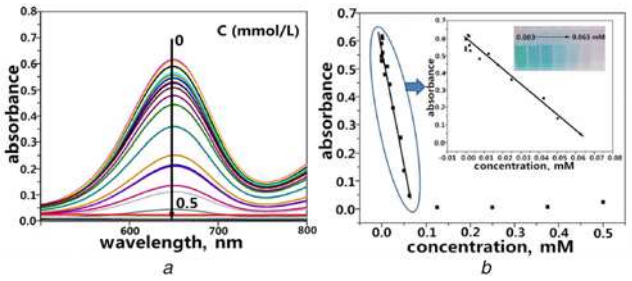

Fig. 5 *Detection of Fe^{2+}*
a UV–Vis absorption of sensing solution at different concentration of Fe^{2+}
b Plots of A_{652} versus the concentration of Fe^{2+}

The limit of detection (LOD) is calculated to be 0.5 µM (LOD = 3 σ/k, where σ, k are the relative standard deviation (RSD) of ten parallel controlled measurements and the slope of the linear calibration plots, respectively), which is lower than the environmental protection agency guideline (5.37 µM) in drinking water and the linear range meets the needs of detection in our daily life. In addition, we compared the sensor based on $MnSiO_3$ NPs with the colorimetric, electrochemical, and fluorescent assays for Fe^{2+} reported previously, $MnSiO_3$ NPs had a lower LOD (Table 1), indicating that this sensor is more sensitive.

The selectivity of this detection method was examined by testing the relative absorbance response towards several possible coexisting substances, including Na^+, Cu^+, Ca^{2+}, $H_2PO_4^-$, K^+, Fe^{3+}, HPO_4^{2-}, HCO_3^-, Zn^{2+}, and so on. As shown in Fig. 6, these species do not produce interference in Fe^{2+} detection.

Table 1 Comparison of this assay with other methods for detection of Fe^{2+}

Methods	Materials used	LOD, µM	Reference
colorimetry	pyridoxal derivative	8.1	[21]
colorimetry	chloroauric acid and L-arginine mixture	20	[22]
colorimetry	Ag NPs	0.54	[23]
colorimetry	amidine	20	[24]
fluorimetry	$Au_7(DHLA)_2Cl_2$ nanoclusters	3.8	[25]
fluorimetry	Ag nanoclusters with poly (methacrylic acid)	3	[26]
electrochemistry	H_2O_2	10	[27]
colorimetry	$MnSiO_3$ NPs	0.5	this work

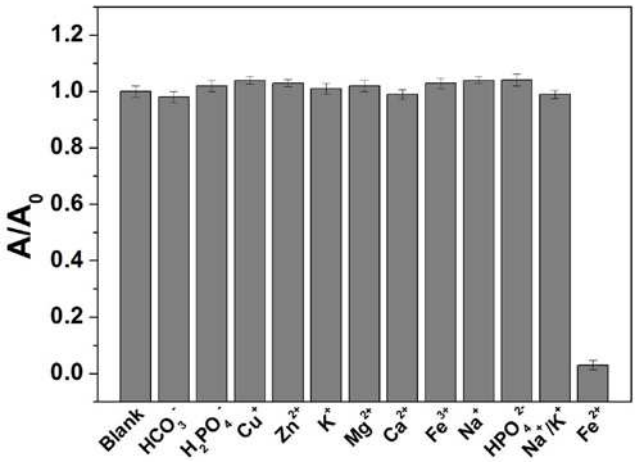

Fig. 6 *Selectivity of Fe^{2+} colorimetric sensing system*

doi: 10.1049/mnl.2019.0543

Table 2 Analytical results for the detection of Fe^{2+} in the lake sample

Sample	Fe^{2+} concentration, μM		Recovery, %	RSD, n=3 %
	Added, μM	Found, μM[a]		
1	25	26.7	106.8	0.19
2	45	45.4	100.8	2.13
3	60	59.5	99.1	0.14

[a]Mean of three determinations.

Thus, the $MnSiO_3$-TMB chromogenic system can provide a reliable visual colorimetric assay for selective detection of Fe^{2+}.

In order to study the feasibility of this method for the detection of Fe^{2+}, different concentrations of Fe^{2+} (25, 45, and 60 μM) were added to the lake water of Zhangjiajie Scenic Area, Hunan. Based on $MnSiO_3$ NPs-TMB system, the content of Fe^{2+} in spiked water samples was calculated. The recoveries are within the range from 99.1 to 106.8% for the three lake water samples, and the RSD is less than 3.0%. As shown in Table 2, it proves that themethod has good practicability for detecting Fe^{2+} and can be used for detecting the content of Fe^{2+} in the real-world samples.

4. Conclusion: In summary, $MnSiO_3$ NPs were prepared by a simple precipitation method, these $MnSiO_3$ NPs were found to exhibit oxidase-like activity. The mechanism is proposed. In acidic media, the proposed low-cost $MnSiO_3$-TMB detection system exhibited good sensitivity and high selectivity. On this basis, a simple and sensitive colorimetric assay for Fe^{2+} in lake water was developed and as low as 3 μM Fe^{2+} could be detected using this method. The oxidase-like activity of $MnSiO_3$ presents a great potential applications in biosensing, biocatalysis, and environment monitoring. There are also some shortcomings to this Fe^{2+} sensor, such as not a continuous analysis.

5. Acknowledgments: This work was financially supported by the National Natural Science Foundation of China (21501106), the Scientific Research Foundation for the Returned Overseas Chinese Scholars and Qingdao Municipal Science and Technology Commission (16-5-1-86-jch), Chemistry Faculty Talents Foundation of Qingdao University of Science and Technology.

6 References

[1] Gao X.H., Lu Y.Z., J S., *ET AL.*: 'Colorimetric detection of iron ions (III) based on the highly sensitive plasmonic response of the N-acetyl-l-cysteine-stabilized silver nanoparticles', *Analytica Chimica Acta*, 2015, **879**, pp. 118–125 (doi: 10.1016/j.aca.2015.04.002)

[2] Sun Y.J., Luo M.C., Meng X.X., *ET AL.*: 'Graphene/intermetallic PtPb nanoplates composites forBoosting electrochemical detection of H_2O_2 released from cells', *Anal. Chem.*, 2017, **89**, pp. 3761–3767 (doi: 10.1021/acs.analchem.7b00248)

[3] Wu D., Zou Z., Lu X., *ET AL.*: '3D conductive NiCo/NiCoOx hybrid nanoclusters modified with amorphous FeOOH nanosheets for sensitive nonenzymatic glucose sensor', *J. Mater. Sci.*, 2019, **54**, pp. 10695–10704 (doi: 10.1007/s10853-019-03662-x)

[4] Sui N., Li S., Wang Y.K., *ET AL.*: 'Etched PtCu nanowires as a peroxidase mimic for colorimetric determination of hydrogen peroxide', *Microchimica. Acta*, 2019, **186**, p. 8 (doi: 10.1007/s00604-019-3293-0)

[5] Frey A., Meckelein B., Externest D., *ET AL.*: 'A stable and highly sensitive 3,3′,5,5′-tetramethylbenzidine-based substrate reagent for enzyme-linked immunosorbent assays', *J. Immunological Meth.*, 2015, **233**, pp. 47–56 (doi: 10.1016/S0022-1759(99)00166-0)

[6] Josephy P.D., Eling T., Mason R.P.: 'The horseradish peroxidase-catalyzed oxidation of 3,5,3′,5′-tetramethylbenzidine. Free radical and charge-transfer complex intermediates', *J. Biol. Chem.*, 1982, **257**, pp. 3669–3675

[7] Chan Y.H., Jin Y.H., Wu C.F., *ET AL.*: 'Copper(II) and iron(II) ion sensing with semiconductingpolymer dots', *Chem. Commun.*, 2011, **47**, pp. 2820–2822 (doi: 10.1039/C0CC04929H)

[8] Chen H., Ren J.: 'Selective detection of Fe^{2+} by combination of $CePO_4$:Tb^{3+} nanocrystal–H_2O_2 hybrid system with synchronous fluorescence scan technique', *Analyst*, 2012, **137**, pp. 1899–1903 (doi: 10.1039/C2AN16202D)

[9] Sun Y., Tan H., mand N., *ET AL.*: 'Sensitive determination of Hg(II) based on a hybridization chain recycling amplification reaction and surface-enhanced Raman scattering on gold nanoparticles', *Microchimica. Acta*, 2018, **185**, p. 363 (doi: 10.1007/s00604-018-2907-2)

[10] Wang H.Y., Wang Y.Y., Bai X., *ET AL.*: 'Manganese silicate drapes as a novel electrode material for supercapacitors', *Rsc Adv.*, 2016, **6**, pp. 105771–105779 (doi:10.1039/C6RA19102A)

[11] Lei Z.B., Zhang J.T., Zhao X.S.: 'Ultrathin MnO_2 nanofibers grown on graphitic carbonspheres as high-performance asymmetric supercapacitorelectrodes', *J. Mater. Chem.*, 2012, **22**, pp. 153–160 (doi: 10.1039/C1JM13872C)

[12] Grosvenor A.P., Bellhouse E.M., Korinek A., *ET AL.*: 'XPS and EELS characterization of Mn_2SiO_4, $MnSiO_3$ and $MnAl_2O_4$', *Appl. Surf. Sci.*, 2016, **379**, pp. 242–248 (doi: 10.1016/j.apsusc.2016.03.235)

[13] Xie S., Guo X.N., Jin G.Q., *ET AL.*: 'Carbon coated Co–Sic nanocomposite with high-performance microwave absorption', *Phys. Chem. Chem. Phys.*., 2013, **15**, pp. 16104–16110 (doi: 10.1039/C3CP52735B)

[14] Aust S.D., Morehouse L.A., Thomas C.E.: 'Role of metals in oxygen radical reactions', *J. Free Radicals in Biol. Med.*, 1985, **1**, pp. 3–25 (doi: 10.1016/0748-5514(85)90025-X)

[15] Vanwinkle B.A., Bentley K.L.D., Malecki J.M., *ET AL.*: 'Nanoparticle (NP) uptake by type I alveolar epithelial cells and their oxidant stress response', *Nanotoxicology.*, 2009, **3**, pp. 307–318 (doi: 10.3109/17435390903121949)

[16] Halliwell B., Gutteridge J.M.: '[1] role of free radicals and catalytic metal ions in human disease: an overview', *Meth. Enzymol.*, 1990, **186**, pp. 1–85 (doi: 10.1016/0076-6879(90)86093-B)

[17] Hancock J.T., Desikan R., Neil S.J.: 'Role of reactive oxygen species in cell signalling pathways', *Biochemical Soc. Trans.*, 2001, **29**, (2), pp. 345–349 (doi: 10.1042/bst0290345)

[18] Yinqiu L.C.S.: 'Study on relationship among transmittance error, absorbance error and absorbance truce value', *Mod. Sci. Instrum.*, 2000, **1**, pp. 35–37

[19] Sloane H.J., Gallaway W.S.: 'Spectrophotometric accuracy, linearity and adherence to beer's law', *Appl. Spectrosc.*, 1977, **31**, pp. 25–30 (doi:10.1366/000370277774463210)

[20] Bastían R.: 'Differential spectrophotometric determination of high percentages of nickel', *Anal. Chem.*, 1951, **23**, pp. 580–586 (doi:10.1021/ac60052a010)

[21] Rana D., Rana A.M., Sahoo S.K.: 'Cation sensing of pyridoxal derived sensors towards Fe (II) Ion in pure aqueous solution', *Chem. Sci. J.*, 2017, **8**, p.177 (doi: 10.4172/2150-3494.1000177)

[22] Qin H., Liao C., Zhang Y., *ET AL.*: 'Colorimetric sensor array for detection of iron (II) Ion', *Current Org. Chem.*, 2018, **22**, pp. 831–834 (doi: 10.2174/1385272821666171002122854)

[23] Basiri S., Mehdinia A., Jabbari A.: 'A sensitive triple colorimetric sensor based on plasmonic response quenching of green synthesized silver nanoparticles for determination of Fe^{2+}, hydrogen peroxide, and glucose', *Colloids Surf. A, Physicochem. Eng. Aspects.*, 2018, **545**, pp. 138–146 (doi: 10.1016/j.colsurfa.2018.02.053)

[24] Nandre J., Patil S., Patil P., *ET AL.*: 'The amidine based colorimetric sensor for Fe^{3+}, Fe^{2+}, and Cu^{2+} in aqueous medium', *J. Fluoresc.*, 2014, **24**, pp. 1563–1570 (doi: 10.1007/s10895-014-1438-4)

[25] Yang L., Chen J., Huang T., *ET AL.*: 'Red-emitting Au_7 nanoclusters with fluorescence sensitivity to Fe^{2+} ions', *J. Mater. Chem. C*, 2017, **5**, pp. 4448–4454 (doi: 10.1039/C7TC00724H)

[26] Cao X., Bai Y., Li F., *ET AL.*: 'One-pot synthesis of highly fluorescent poly (methacrylic acid)-capped silver nanoclusters for the specific detection of iron (II)', *ChemistrySelect.*, 2019, **4**, pp. 12183–12189 (doi:10.1002/slct.201903673)

[27] Jia S., Liang M., Guo L.H.: 'Photoelectrochemical detection of oxidative DNA damage induced by Fenton reaction with low concentration and DNA-associated Fe^{2+}', *J. Phys. Chem. B.*, 2008, **112**, pp. 4461–4464 (doi:10.1021/jp711528z)